

Combined evaluation of MPI-ESM land surface water and energy fluxes

Stefan Hagemann¹, Alexander Löw¹ and Axel Andersson²

(stefan.hagemann@zmaw.de)

¹) Max Planck Institute for Meteorology (MPI-M), ²) German Weather Service, Offenbach

Abstract

In order to assess the robustness of projected changes in the hydrological cycle simulated by an Earth System Model (ESM), it is fundamental to validate the ESM and to characterize its major deficits. As the hydrological cycle is closely coupled to the energy cycle, a common large-scale evaluation of these fundamental components of the Earth system is highly beneficial, even though this has been rarely done up to now. Thus, Hagemann et al. (2013) performed a combined evaluation of land surface water and energy fluxes from the newest ESM version of MPI-M, MPI-ESM, which was used to produce an ensemble of CMIP5 simulations. Observations comprise WATCH forcing data (WFD; Weedon et al. 2011), MODIS surface albedo (Schaaf et al. 2002) and surface solar irradiance (SSI) from CERES (Loeb et al. 2012) and CMSAF (Müller et al. 2009). Additionally, MPI-ESM results are compared to CMIP3 results from the predecessor of MPI-ESM, ECHAM5/MPIOM, as well as to results from the atmosphere/land part of MPI-ESM (ECHAM6/JSBACH) forced by observed SST. The analyses focus on regions where notable differences occur between the two ESM versions as well as between coupled and SST driven simulations. **Table 1** gives an overview on all simulations considered.

Table 1

GCM	MPI-ESMh	ECHAM5h	MPI-ESMa	ECHAM5a
Model Version	ECHAM6/MPIOM Historical runs CMIP5 3 member ensemble mean	ECHAM5/MPIOM IPCC AR4 CMIP3 3 member ensemble mean	ECHAM6 AMIP2 forcing, 3 member ens. mean	ECHAM5 AMIP2 forcing
Time	1971-2000	1971-2000	1979-2000	1979-1999
Resolut.	T63L47/GR15L40	T63L31/GR15L40	T63L47	T63L31

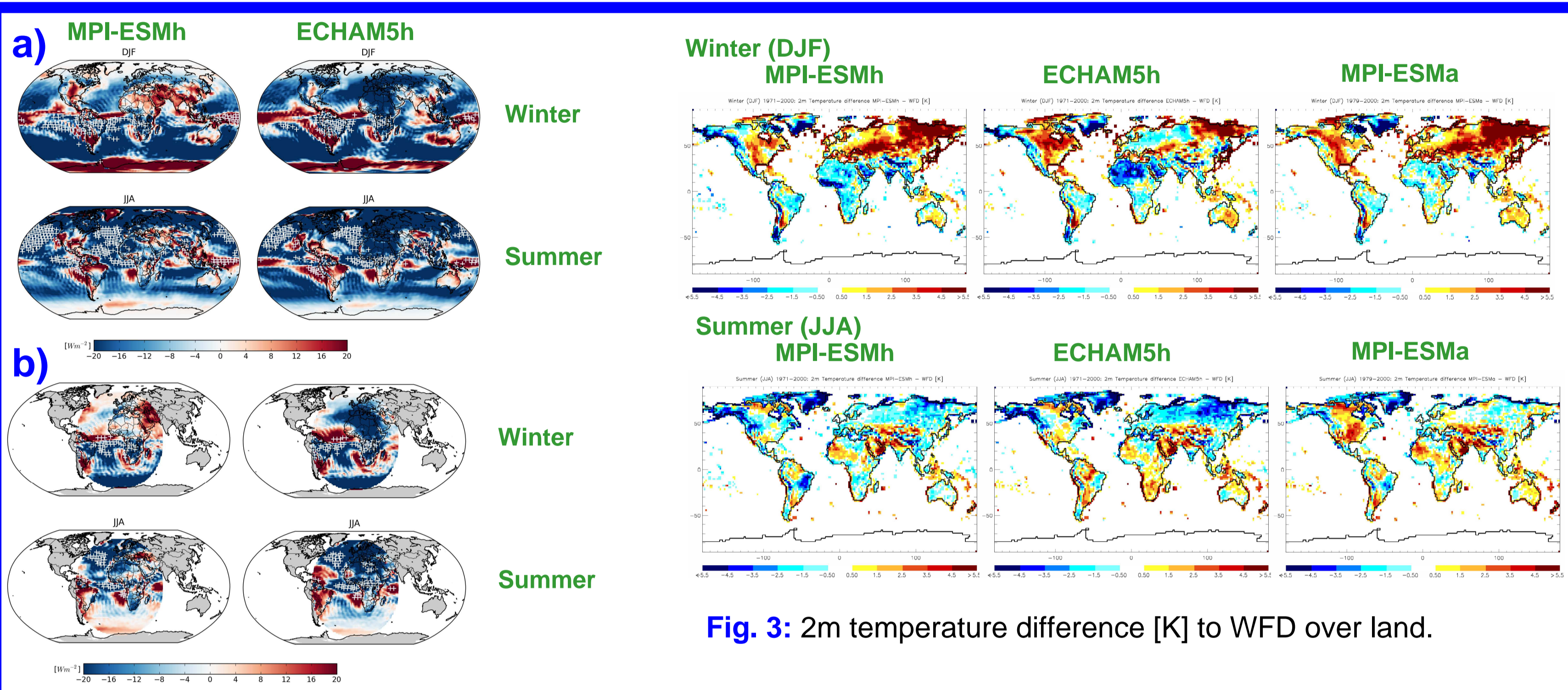


Fig. 1: SSI differences [W/m²] of MPI-ESMh and ECHAM5h to a) CERES (2000-2003) and b) CMSAF (1989-2005) data.

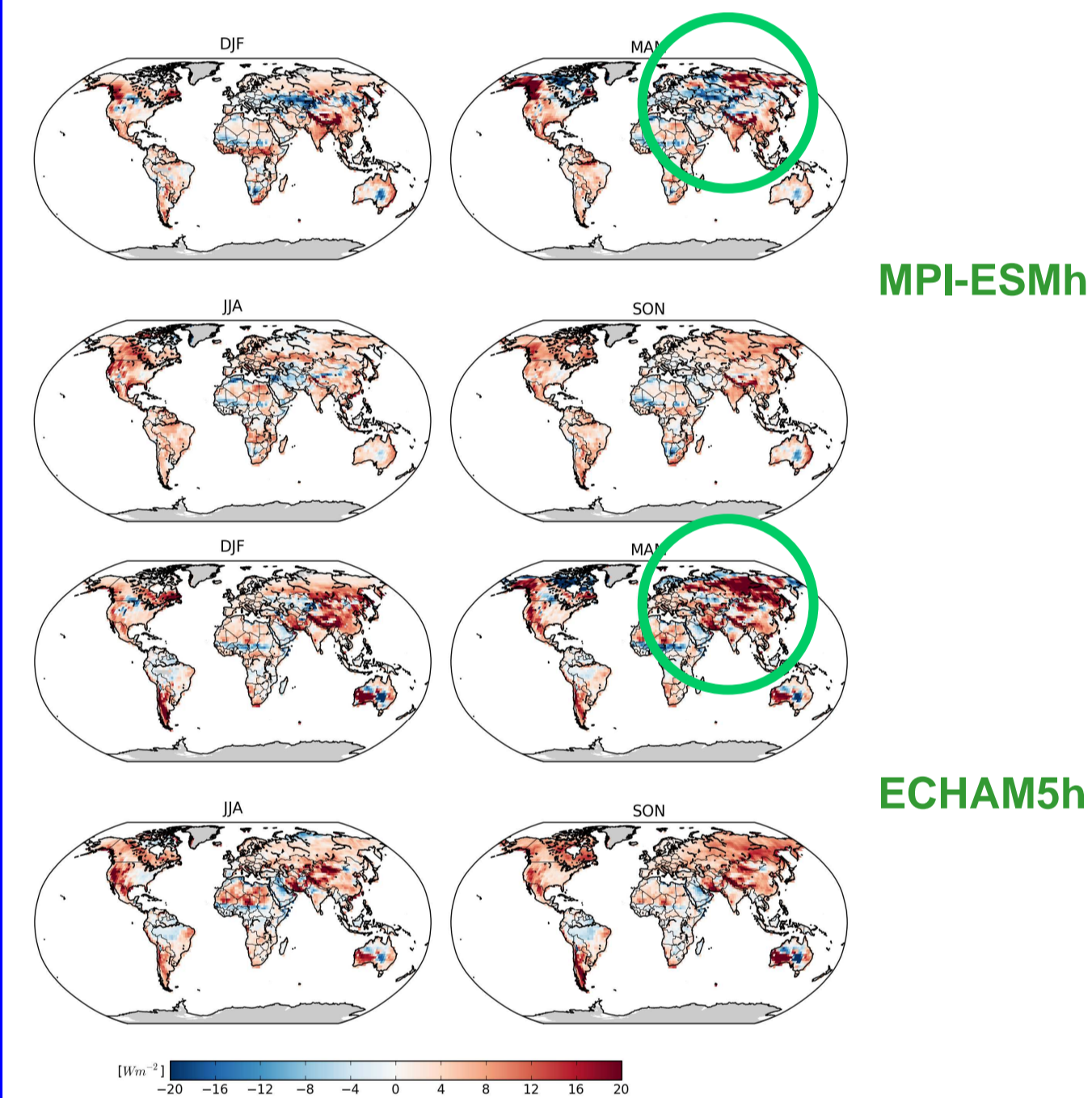


Fig. 2: Seasonal differences in upward shortwave flux [W/m²] compared to MODIS data (2001-2010), representing albedo scaled with model incoming radiation for MPI-ESMh (top) and ECHAM5h (bottom).

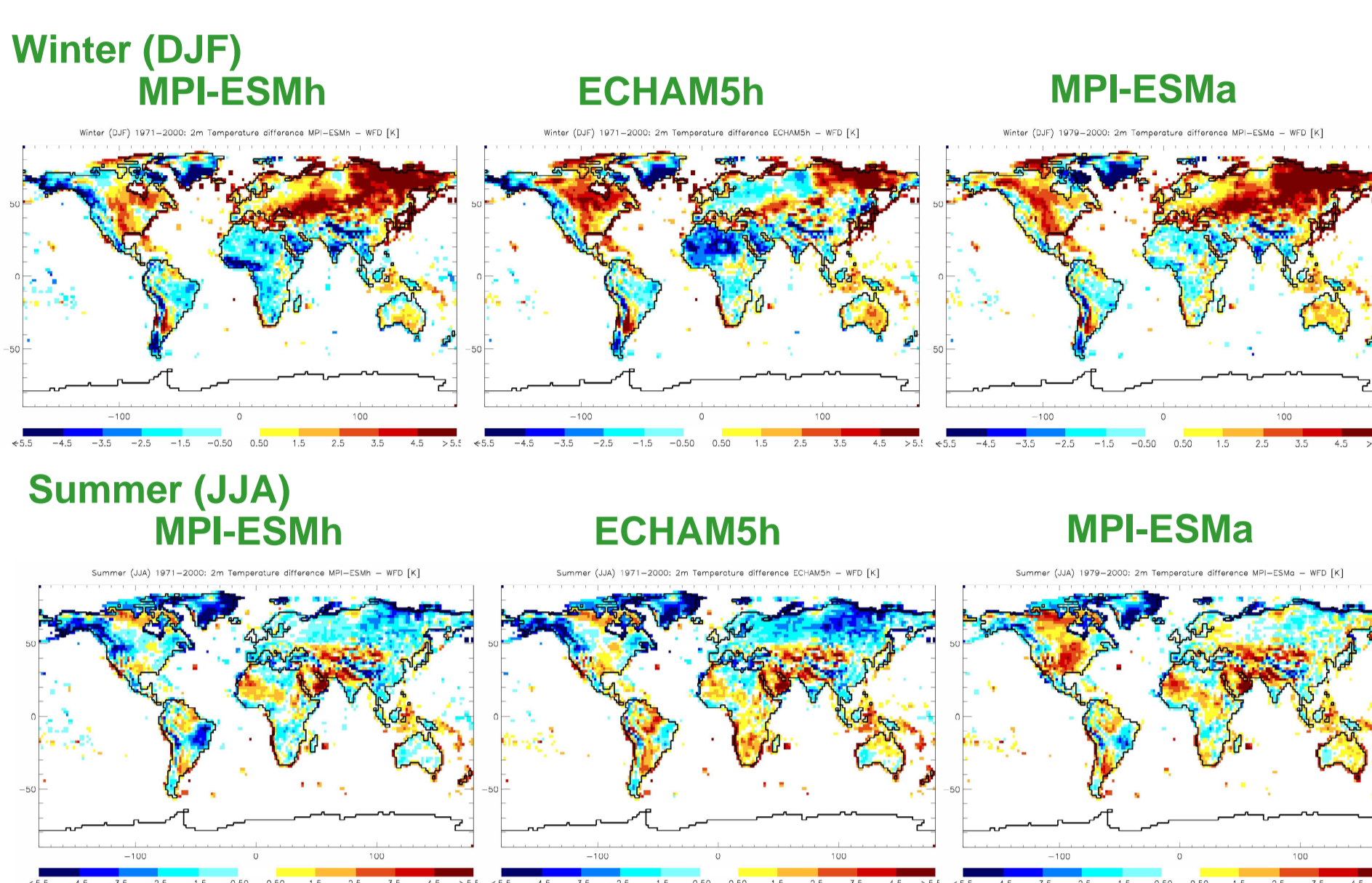


Fig. 3: 2m temperature difference [K] to WFD over land.

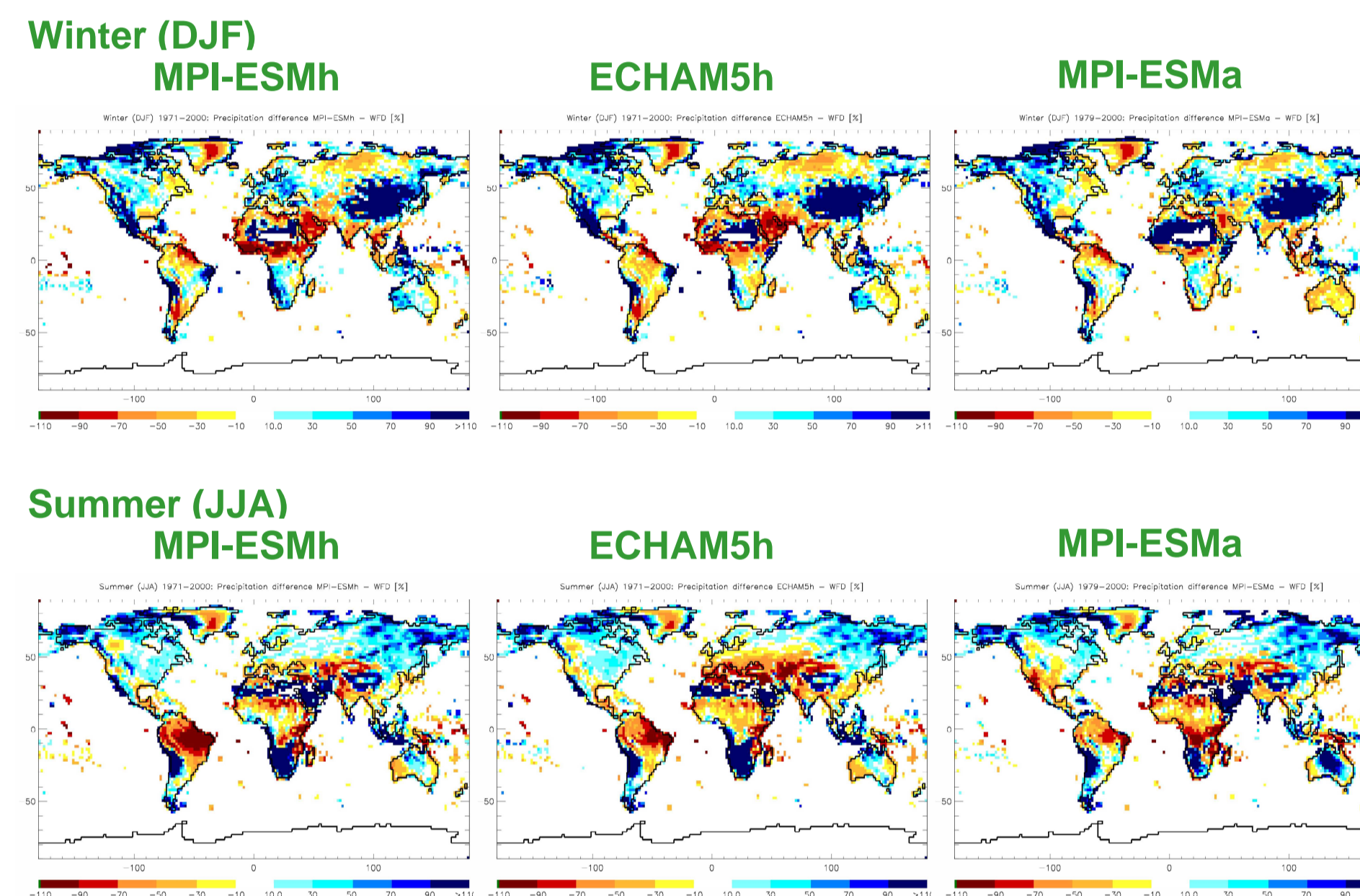


Fig. 4: Relative precipitation difference [%] to WFD over land.

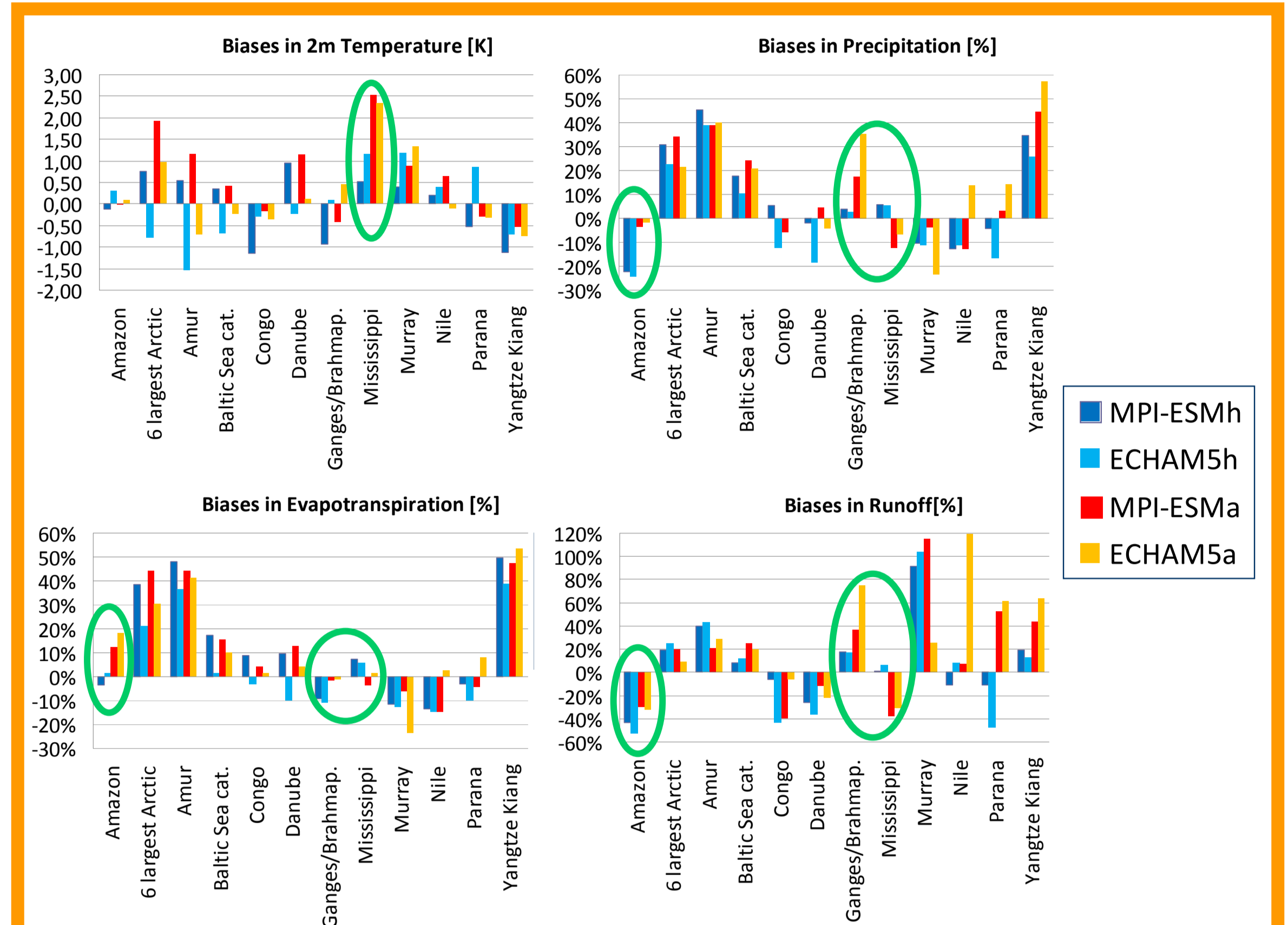


Fig. 5: Biases in the water balance (upper panel) and the 2m temperature (lower panel) over selected large catchments of the globe. Observations comprise WFD and observed climatological discharge.

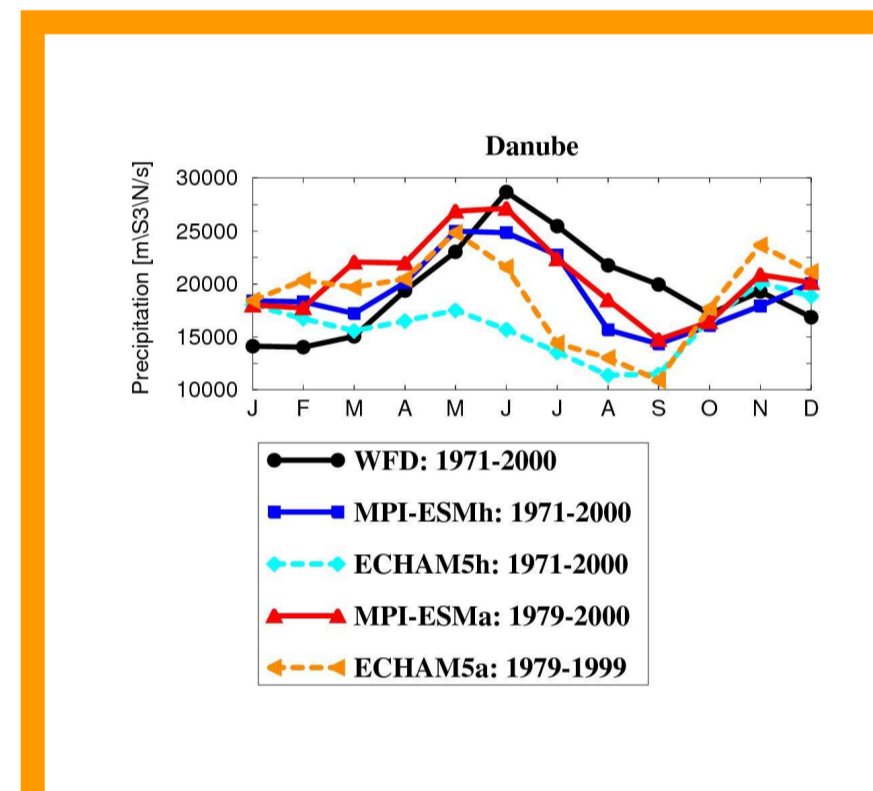


Fig. 6 Simulated and observed precipitation [m³/s] over the Danube catchment.

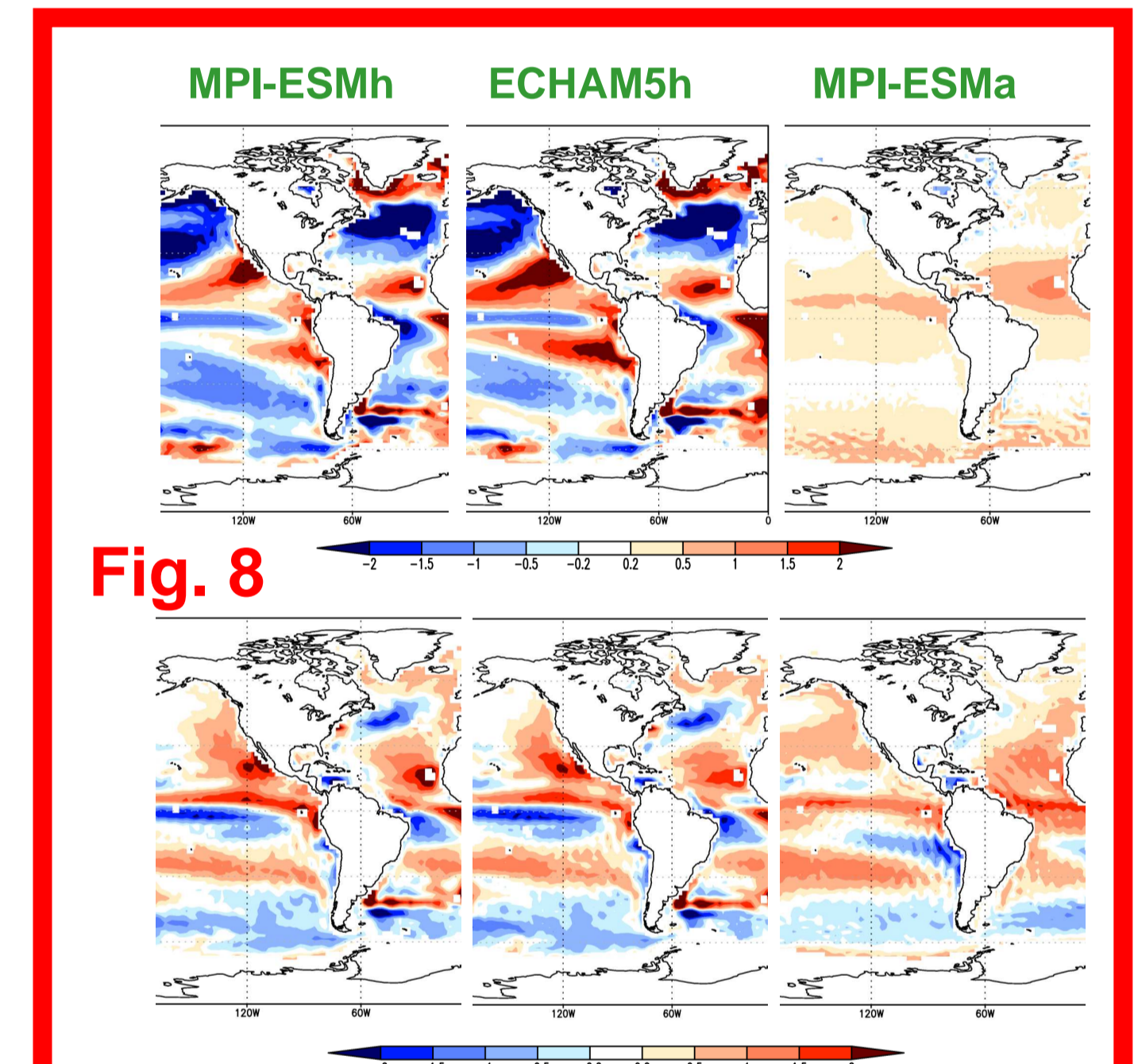
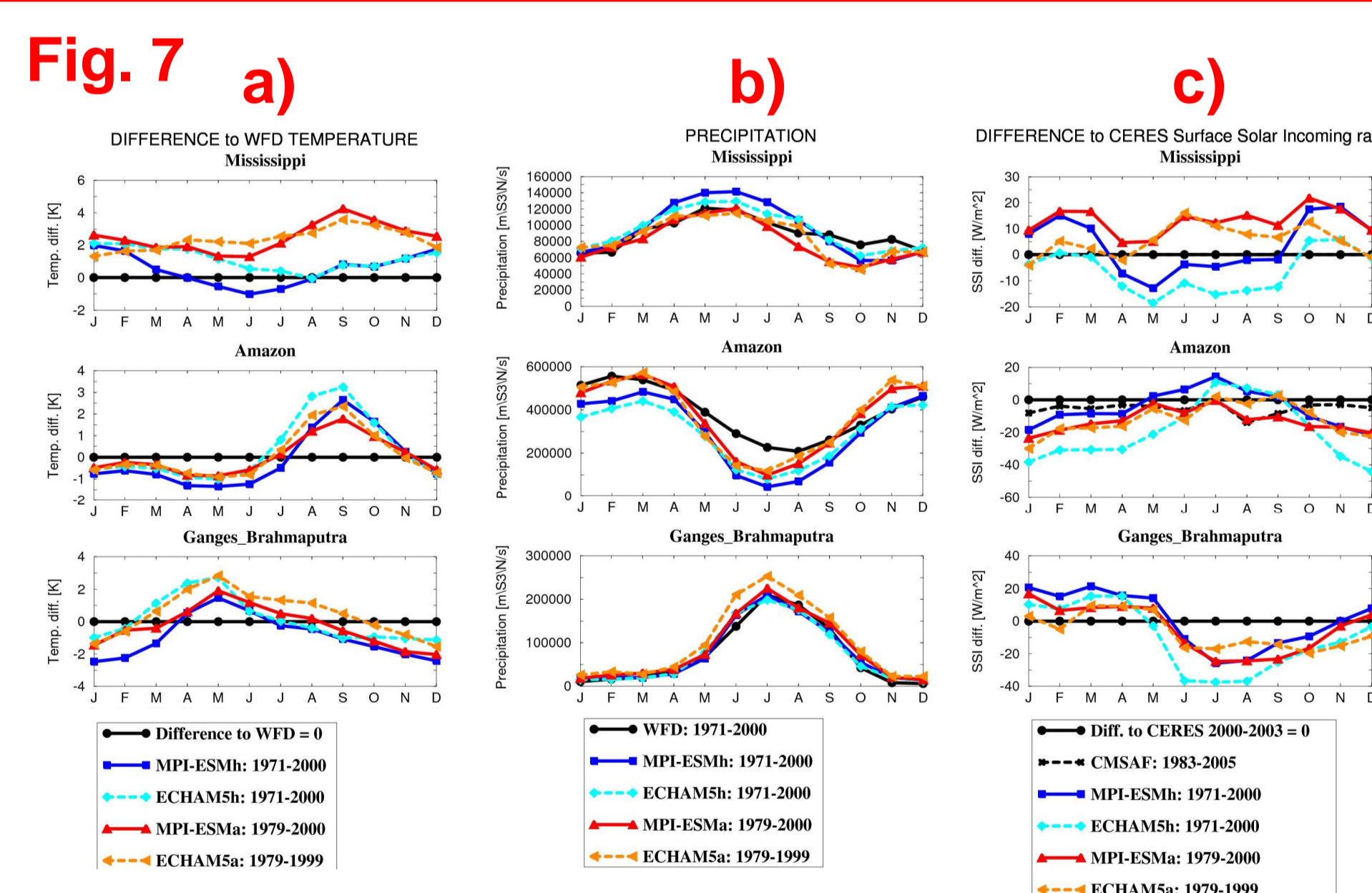


Fig. 8



Summary

- Considerably reduced bias of simulated SSI (Fig. 1) and surface albedo (Fig. 2) in MPI-ESM simulations compared to ECHAM5
- This leads to subsequent differences in simulated 2m temperature (Fig. 3).
- For the hydrological cycle, large-scale bias patterns are rather similar between the different models over many regions (Fig. 4 and Fig. 5), except:
 - Summer drying problem is largely reduced in MPI-ESM runs over the Danube (Fig. 6).
 - Coupling to ocean leads to improved precipitation over Ganges/Brahmaputra and Mississippi catchments, but to a dry bias over the Amazon (Fig. 7).
- Mississippi (Fig. 8):** Warm bias of coupled simulations in the Tropical Atlantic leads too enhanced evaporation over the ocean and enhanced moisture transport into the catchment, thereby compensating a dry bias that is likely land surface related.
- Amazon (Fig. 9):** In the coupled simulations, biases in the SST pattern (e.g. low bias at Brazilian coast) and associated moisture transport (low atmospheric moisture and too low wind speed at NE coast) cause the dry bias throughout the year. The dry bias during the boreal summer, which is persistent in all models, is probably caused by an insufficient representation of land surface processes.
- Ganges/Brahmaputra (Fig. 10):** Missing interaction of the ocean with the atmosphere over the Arabian Sea causes overly strong evaporation in the SST forced simulations. The excess moisture is transported into the catchment causing the too enhanced precipitation.



Comparing coupled & AMIP2-SST forced ESM simulations

Fig. 7: a) Differences to WFD 2m temperature [K], b) simulated and observed precipitation [m³/s], and c) differences to CERES SSI [W/m²] over Mississippi, Amazon and Ganges/Brahmaputra catchments.

Fig. 8: Summer (JJA) SST (upper row) and evaporation (lower row) differences to HOAPS data (1989-2005).

Fig. 9: Annual mean SST (upper row) and integrated water vapour (lower row) differences to HOAPS data (1989-2005).

Fig. 10: Summer (JJA) SST (upper row) and evaporation (lower row) differences to HOAPS data (1989-2005).

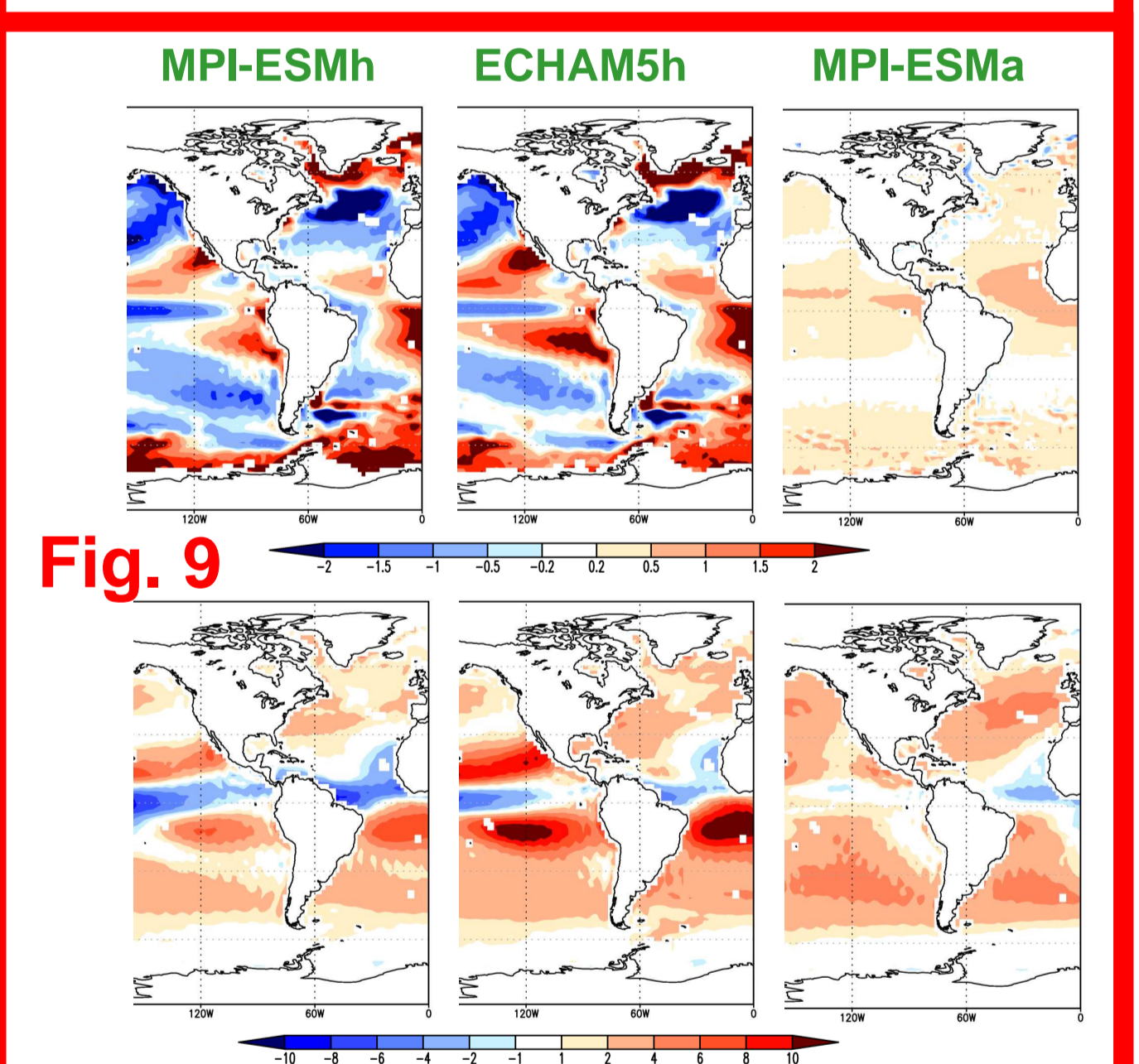


Fig. 9

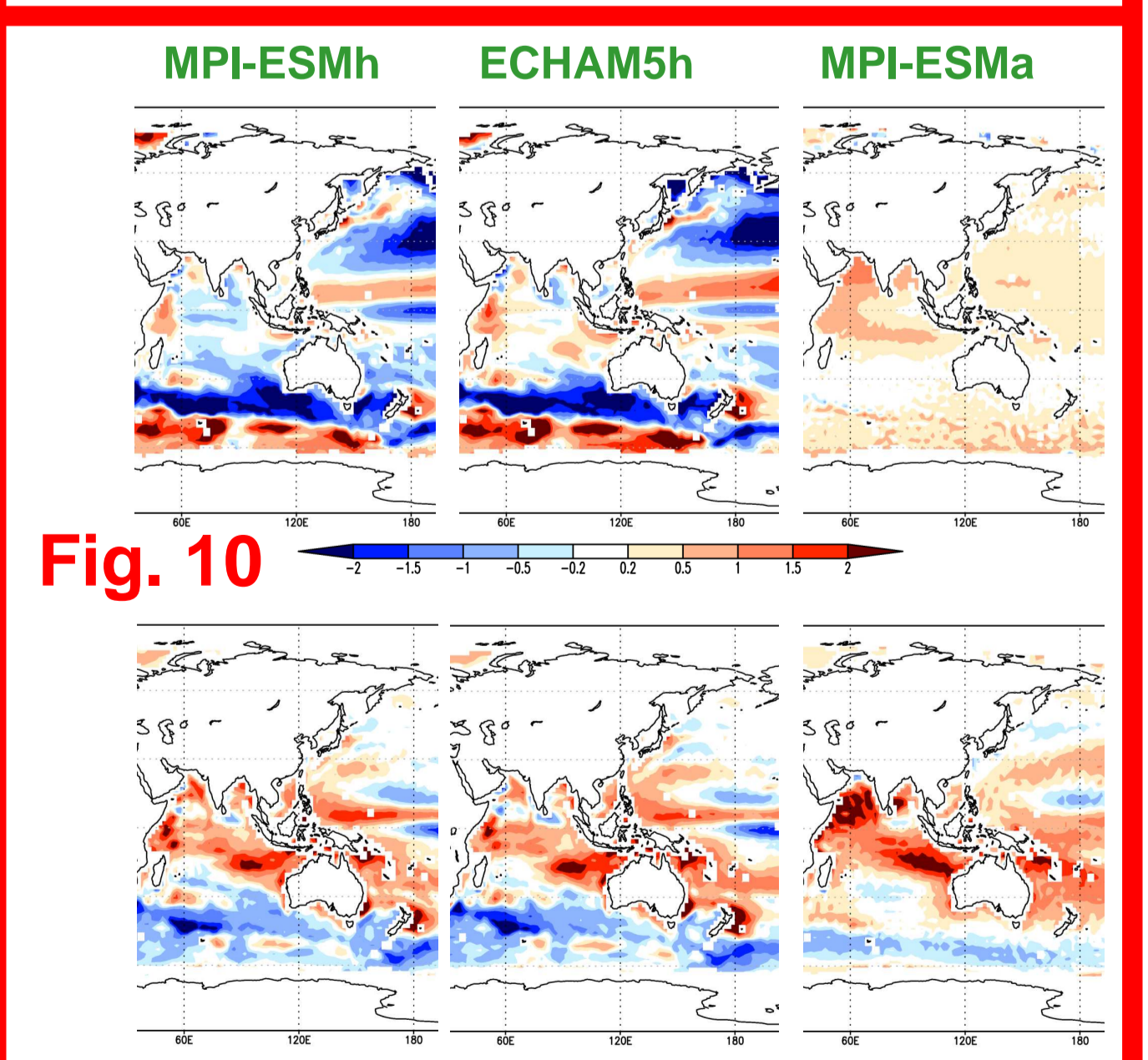


Fig. 10

References

- Hagemann, S., A. Loew, A. Andersson (2013) Combined evaluation of MPI-ESM land surface water and energy fluxes. *J. Adv. Model. Earth Syst.*, doi:10.1029/2012MS00173, in press.
- Loeb, N. G., et al. (2012), Advances in understanding top-of-atmosphere radiation variability from satellite observations, *Surveys in Geophysics*, doi: 10.1007/s10712-012-9175-1.
- Müller, R. W., et al. (2009) The CMSAF operational scheme for the satellite based retrieval of solar surface irradiance - A LUT based eigenvector hybrid approach. *Remote Sens. of Environ.*, 113 (5), 1012-1024.
- Schaaf, C. B., et al. (2002) First Operational BRDF, Albedo and Nadir Reflectance Products from MODIS, *Remote Sens. Environ.*, 83, 135-148.
- Weedon, G.P., et al. (2011) Creation of the WATCH forcing data and its use to assess global and regional reference crop evaporation over land during the twentieth century. *J. Hydrometeorol.*, 12, 823-848.